Interfacial Synthesis

DOI: 10.1002/anie.200907120

Luminescent Ag_7 and Ag_8 Clusters by Interfacial Synthesis**

*T. Udaya Bhaskara Rao and T. Pradeep**

Dedicated to Professor Manjanath Subraya Hegde on the occasion of his 65th birthday

Molecular quantum clusters of noble metals are a fascinating area of contemporary interest in nanomaterials. While Au_{11},[1] Au_{13},[2] and Au_{55}[3] have been known for a few decades, several new clusters were discovered recently. These include Au_8,[4] Au_{18},[5] Au_{25},[6] Au_{38},[7] and so on. Au_{11} has also been the subject of recent research.[8] In view of their luminescence, several of these clusters are expected to be important in biolabeling[9] and fluorescence resonance energy transfer[6f] as well as for creating luminescent patterns.[10] There are many examples of template-assisted synthesis of water-soluble luminescent silver clusters[11] with cores ranging from Ag_2 to Ag_8, having characteristic electronic transitions between 400–600 nm. However, unlike the case of gold, there are only limited examples of monolayer-protected silver analogues. Silver clusters protected with aryl,[12] aliphatic,[13] and chiral[14] thiols have been reported, some of which have characteristic optical[12b,13,14c] and mass spectrometric[12a,13,14c] signatures. There is also a family of well-characterized metal-rich silver chalcogenide clusters.[15] Besides single-crystal diffraction,[15] mass spectrometry[15c,e] has also been used for detailed understanding of these clusters. Ag^I clusters with[16] and without[17] luminescence have also been reported. Herein we present gram-scale syntheses of two luminescent silver clusters, protected by small molecules containing thiol groups, with well-defined molecular formulas, by interfacial synthesis. This new synthetic approach has become promising in several other areas including semiconductor nanoparticles, two-dimensional superlattices, and 3D structures.[18]

A crude mixture of red- and blue-green-emitting clusters $Ag_8(H_2MSA)_8$ and $Ag_7(H_2MSA)_7$ (H_2MSA: mercaptosuccinic acid), respectively, was synthesized in gram quantities by an interfacial etching reaction conducted at an aqueous/organic interface starting from H_2MSA-protected silver nanoparticles ($Ag@H_2MSA$)[19] as precursor (for details see the Experimental Section and Figure S1 in the Supporting Information). During the reaction, the optical absorption spectrum of the aqueous phase showed gradual disappearance of the surface plasmon resonance at 400 nm (Figure 1 A) of metallic silver nanoparticles. The color of the aqueous phase gradually changed from brown to yellow and finally to orange. The particles of Ag@MSA are polydisperse (Figure 1 Ca) and form smaller clusters in the aqueous phase upon etching (Figure 1 Cb) with complete disappearance of the nanoparticles. The unetched particles move to the junction of the two phases and form a self-assembled film of monodisperse nanoparticles, resembling two-dimensional superlattices (Figure 1 Cc), which appears blue in color. The smaller clusters formed in the reaction upon longer electron-beam irradiation coalesce to form nanoparticles (Figure S2). It is known that such clusters are unstable to high-energy electrons.[6e]

The peak at 600 nm, which appears at shorter reaction time (60 min) and may be due to interplasmon coupling, disappears slowly, and a new feature is seen at 550 nm after 48 h of reaction (Figure 1 A). In accordance with previous studies on silver clusters, we assign this peak to interband

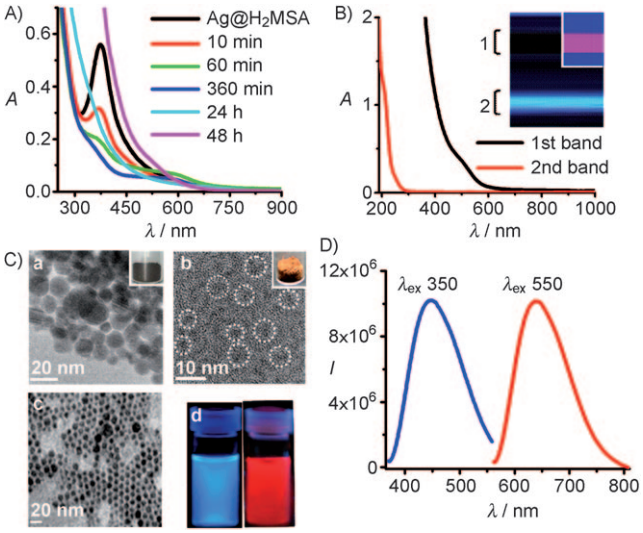

Figure 1. A) Time-dependent UV/Vis spectra of the clusters synthesized during interfacial etching at room temperature. B) UV/Vis absorption spectra of the clusters obtained from the two bands in PAGE. The inset shows a photograph of the wet gel after electrophoresis in UV light at room temperature, and the inset to the inset an image of the first band at 273 K. C) HRTEM images of a) as-synthesized Ag@(H_2MSA), b) the product obtained after interfacial etching, and c) particles in the blue layer at the interface. Individual clusters are not observable by TEM, but aggregates are seen faintly (b, shown in circles). Insets of (a) and (b) are photographs of Ag@MSA and crude cluster samples. d) Photographs of aqueous of cluster solutions of first (cluster 1) and second (cluster 2) PAGE bands at 273 K and room temperature, respectively. D) Luminescence emission of cluster 1 and cluster 2 in water, excited at 550 and 350 nm, respectively.

[*] T. Udaya Bhaskara Rao, Prof. T. Pradeep
DST Unit of Nanoscience (DST UNS), Department of Chemistry and Sophisticated Analytical Instrumentation Facility
Indian Institute of Technology Madras, Chennai 600036 (India)
E-mail: pradeep@iitm.ac.in

[**] We thank the Department of Science and Technology, Government of India for constantly supporting our research program on nanomaterials.

Supporting information for this article is available on the WWW under http://dx.doi.org/10.1002/anie.200907120.

transitions between orbitals derived from the 4d valence band and 5sp conduction band. Templated Ag_n clusters[11] and monolayer-protected clusters[12–14] show interband transitions between 400 and 600 nm. Thus, during interfacial etching, the size of silver nanoparticles is clearly reduced below the Fermi wavelength of the electron, so that a plasmon band at about 400 nm and continuous density of states disappear and discrete energy levels leading to molecular absorption appear. The orange powder separated from the aqueous phase after 48 h of etching exhibits red emission in the solid and solution states. This crude mixture was separated into differently sized clusters by polyacrylamide gel electrophoresis (PAGE). Electrophoresis showed two bands, which indicated the presence of two different clusters. The first band (cluster 1) was red and the second band (cluster 2) was light yellow in visible light, the latter does not appear clearly. The bands are, however, seen clearly in UV, cluster 1 is pink at 273 K and cluster 2 is blue-green at room temperature (inset of Figure 1B). These bands were separated and the free clusters collected in water. Cluster 1 has a characteristic optical absorption signature at 550 nm, in agreement with that of the crude product, while cluster 2 has no distinguishable feature in the visible region (Figure 1B). Cluster 2 emits observable blue-green luminescence at room temperature. The red luminescence of cluster 1 is observable to naked eye only at low temperatures ($\leq$273 K). The emission spectra of clusters 1 and 2 show sharp maxima at 650 and 440 nm, with excitation maxima of 550 and 350 nm, respectively. No qualitative change was seen in the optical absorption spectrum at low temperature. The quantum yields calculated for cluster 1 in water at room temperature and at 273 K are 0.3 and 9%, respectively. The enhancement in emission even with a small decrease in temperature is significant, and this enabled photographing the solutions at lower temperatures. A very large enhancement of this kind in a narrow temperature window is interesting and may result in a range of applications for this material. The solid-state emission is broad and slightly redshifted compared to the solution state, as expected (Figure S3).

Confirmation of the molecular formulas came from mass spectrometric studies with soft ionization techniques such as electrospray ionization (ESI) and matrix-assisted laser desorption ionization (MALDI). Supporting evidence (see below) was obtained by X-ray photoelectron spectroscopy (XPS), energy-dispersive analysis of X-rays (EDAX), and elemental analysis. The matrix DCTB (*trans*-2-[3-(4-*tert*-butylphenyl)-2-methyl-2-propenyldidene]malononitrile) is known to give intact molecular species from metal clusters in MALDI MS.[20a] The MALDI MS data of clusters 1 and 2 are presented in Figure 2. From such fragile species, in view of the fragmentation of the C–S bond upon laser impact,[20b] a variety of gas-phase clusters are also expected. The spectra were therefore compared with those obtained by laser desorption ionization (LDI). The LDI MS spectra (Figure 2) show a series of $Ag_nS_m^-$ species (marked with *) with characteristic spacing. The MALDI MS spectra, however, show additional features due to the intact clusters, which can be assigned to the species $[Ag_8(H_2MSA)_4(HMSA)_4]^-$ and $[Ag_7(H_2MSA)_5(HMSA)_2]^-$ for clusters 1 and 2, respectively.

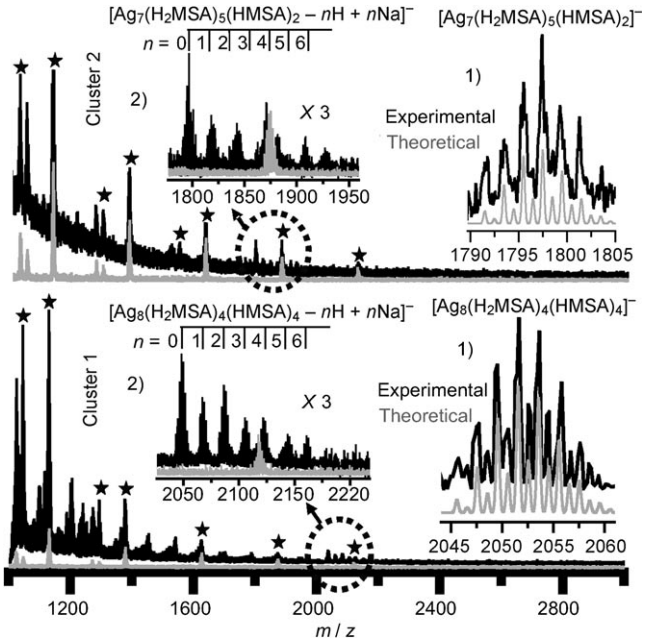

Figure 2. Comparison of the negative-ion MALDI (black) and LDI MS (gray) data of clusters 1 (bottom) and 2 (top). The $Ag_nS_m^-$ series is marked in each trace with asterisks. The intact-ion pattern is compared with the theoretical spectrum in inset 1. Inset 2 shows the Na adducts of formulas, $[Ag_7(H_2MSA)_5(HMSA)_2 - nH + nNa]^-$ and $[Ag_8(H_2MSA)_4(HMSA)_4 - nH + nNa]^-$ ($n = 0, 1, 2, \ldots$).

As MSA is a dicarboxylic acid, it can ionize to give negatively charged species, as well as existing in the form of sodium adducts. Characteristic isotope patterns matching exactly with the theoretical formulas and sodium adducts of the kind $[Ag_8(H_2MSA)_4(HMSA)_4 - nH + nNa]^-$ and $[Ag_7(H_2MSA)_5(HMSA)_2 - nH + nNa]^-$ ($n = 0, 1, 2, \ldots$) are seen for the molecular ions (insets). These ions and their sodium adducts are absent in the LDI MS data. The presence of charged species of the kind $[Ag_7(H_2MSA)_5(HMSA)_2]^-$ suggests the possibility of a charged core, as the overall species is singly charged, in view of the well-defined isotope patterns with separation of m/z 2. For the Ag_8 core, too, although $[Ag_8(H_2MSA)_7(HMSA)]^-$ is expected, we see $[Ag_8(H_2MSA)_4(HMSA)_4]^-$, again due to a charged core or modifications in the ligand structure on ionization. The existence of a charged core in the condensed phase needs additional investigation, although such a core was proposed recently.[13] The MALDI MS data do not show evidence for any species of higher molecular mass up to m/z 100000. In view of these findings, we conclude that clusters 1 and 2 have the formulas $Ag_8(H_2MSA)_8$ and $Ag_7(H_2MSA)_7$, respectively.

Further confirmation came from negative-ion ESI MS measurements on clusters 1 and 2 in water/methanol (50:50) (Figure 3), which showed characteristic signatures due to silver clusters. These features are also seen in the mass spectrum of the crude product of interfacial etching before PAGE separation. Several of the peaks observed in the crude product are also seen in the isolated clusters (marked a–h), and this indicates similarity in the structures of the clusters. This suggests that the lower mass peaks are derived from

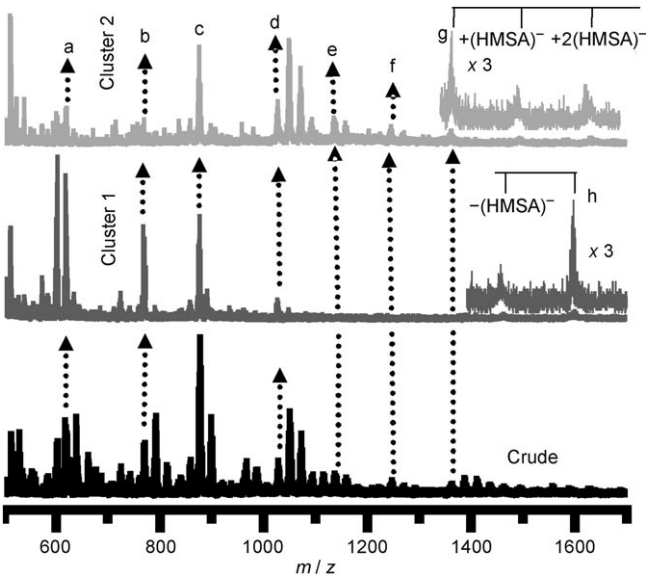

Figure 3. Electrospray ionization mass spectra of crude cluster mixture (bottom), cluster 1 (middle), and cluster 2 (top) in negative ion mode. Specific peaks are labeled as mentioned in text.

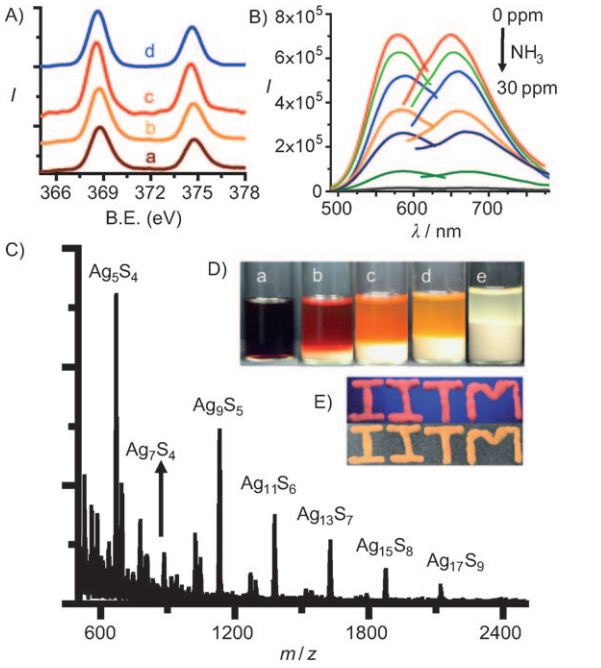

Figure 4. A) Ag 3d XPS spectra of a) the nanoparticles, b) crude cluster, c) Ag_8, d) and Ag_7. B) Luminescence spectra of Ag_8 on addition of ammonia from 5 to 30 ppm. C) LDI mass spectra of Ag_8-loaded alumina. D) Photograph of a concentrated solution of crude cluster in water on addition of various quantities of alumina under white light. E) Photograph of Ag_8-loaded alumina at 0.5 wt% under UV light (top) and under visible light (bottom) at room temperature.

common fragments. Ag_7 and Ag_8 are the heaviest silver-containing species detected in the mass spectra of clusters 1 and 2, respectively. From a detailed analysis of the mass spectrum and CHNS elemental analysis (Figure S4), a chemical composition of $Ag_8(H_2MSA)_8$ can be assigned for the molecular species in band 1 of the gel. The proposal is also in agreement with bulk characterization by EDAX (Figure S5).

The experimentally observed isotope distributions of each fragment (Figure S6) matches perfectly with the calculated pattern. The isotope pattern, as expected, is dominated by silver, with characteristic spacing of m/z 2, which suggests singly charged species. The mass spectrum shows a rich variety. The peaks due to $Ag_4(H_2MSA)_3(HMSA)^-$ (m/z 1027) and $Ag_4(H_2MSA)_2(MSA)^-$ (m/z 877) are in good agreement with the calculated values (1026.6 and 876.6, respectively). Fragmentation of molecular ions resulted in peaks b–d (Figure 3). The sodium adducts give characteristic signatures which are more evident in the crude sample (Figure S6). These precise mass spectral observations coupled with isotope resolution, which is in complete agreement with the theoretical mass spectrum, suggest that $Ag_8(H_2MSA)_8$ is a molecular species existing in solution. Intact $Ag_8(H_2MSA)_8$ is not detected because of the mass limit of the instrument, but the fragments and an atomic ratio of 1:1 for Ag:S from EDAX and XPS analyses confirm this assignment. Mass spectra and EDAX and XPS signatures support the assignment of $Ag_7(H_2MSA)_7$ for cluster 2 as well.

The molecular formula and chemical nature are supported by XPS (Figure S7) and FTIR spectroscopy (Figure S8). XPS survey spectra show all the expected elements. The Ag:S atomic ratio in each case for clusters 1 and 2 is 1:1, in accordance with the molecular formulas. Expanded scans of the specific regions of Ag, C, O, and S were measured. Ag 3d (Figure 4A) shows an Ag^0 value, although a slight binding-energy shift of 0.2 eV could be noticed. S 2p is thiolate-like, and a value of 161.7 eV is observed (Figure S7). This is in agreement with the IR spectrum, which suggests loss of the thiolate proton on cluster formation. Multiple C 1s positions are seen, in accordance with the chemical structure, but surface contamination, which could not be avoided, prevented us from observing the expected ratios for the various C1s features. As the sample is delicate, the usual surface cleaning steps for XPS cannot be performed on the samples. The formation of small clusters in the reaction is further confirmed by the X-ray diffraction pattern, which shows the absence of characteristic peaks exhibited by parent silver nanoparticles of size 5–10 nm (Figure S9). No characteristic peaks were observed for silver clusters formed in microemulsions.[11d]

Our attempts to crystallize these clusters were unsuccessful. To check whether the luminescence originates from the cluster core, we did a core etching reaction with ammonia and cyanide, which are known to etch silver and gold nanoparticles. Both the luminescence and the absorption are instantaneously quenched on addition of NH_3 and CN^-, as shown for the former in Figure 4B (the result for CN^- was similar). Vanishing of absorption and emission of the cluster is due to etching of the cluster core by NH_3 and CN^-. Note that the concentrations of the etching regents were extremely low. This experiment proved that absorption and emission originate from the cluster core.

These clusters were loaded onto metal oxides such as Al_2O_3, MgO, SiO_2, and TiO_2. Gradual color changes on addition of Al_2O_3 to a concentrated solution of the crude cluster in water are shown in Figure 4D. The supernatant solution, after 2 h of soaking, appears pale yellow and emits blue-green under UV light. The change in luminescence profile verses the amount of Al_2O_3 added is given in Figure S10. This shows that only the Ag_8 clusters are adsorbed on metal oxides, leaving the Ag_7 clusters in solution. This difference in affinity and selective adsorption of clusters may be exploited in applications. The LDI-MS spectrum of Ag_8 loaded alumina (Figure 4C) shows characteristic $Ag_nS_m^-$ peaks, as discussed above. The Ag_8-loaded solids exhibit characteristic luminescence at room temperature (Figure 4E).

Luminescence decays of Ag_8 in the solid state and Ag_7 in the solution state were measured by two techniques. The data obtained by a picosecond time-correlated single-photon counting (TCSPC) technique are shown in Figure S11. Lifetimes of Ag_8 clusters were obtained by numerical fitting of the emission at 630 nm. The luminescence decay profile showed four components at 35 ps (97%), 37.2 ns (0.6%), 37.2 ns (1.72%), and 5.68 ns (0.6%). Lifetimes of Ag_7 were obtained by numerical fitting of the emission at 440 nm. The luminescence decay profile showed four components at 0.012 (88.9), 0.396 (4.8), 2.10 (4.8), and 8.31 ns (1.3%). Both clusters show a dominant fast component.

To use these clusters in various studies, it is important that they are transferable to various solvent systems. The solubility of the as-prepared clusters is extremely sensitive to solvent polarity, and they precipitate even in an excess of methanol. We found that the clusters can be phase-transferred completely from water to organic solvents, such as toluene, by using phase-transfer reagents. Photographs of Ag_8 before and after phase-transfer are shown in Figure S12. These phase-transferred clusters can be dried and redissolved in organic media. The luminescence of the clusters was enhanced upon phase transfer. Hydrogen bonding of the cluster with solvent molecules appears to reduce the luminescence intensity, and by protecting it with phase-transfer reagents, the interaction with the solvent is minimized.

There is a systematic dependence of the luminescence intensity on the polarity of the medium. The optical absorption and emission in methanol/water (1/1 v/v) of Ag_8 shows observable luminescence enhancement even at room temperature (Figure S13). Luminescence intensity and emission wavelength of the cluster vary from solvent to solvent. The effect is pronounced and visually observable in the solid state. The PAGE gel without clusters does not show any luminescence under UV light. The dried gel with Ag_8 show a faint color in visible light (Figure S14), but observable emission under UV light. The color changes on wetting with acetone and methanol, but luminescence disappears to the naked eye on sprinkling with water. This is evident from the photograph of the wet gel in Figure 1B. The loss of luminescence is due to the increase in nonradiative processes by the addition of water. The quenched luminescence reappeared on keeping the sample at 273 K or on evaporating water at room temperature. Recently Ras and co-workers reported that metal nanoclusters show drastic changes in the solvatochromic and solvatofluorochromic properties with varying environment.[11g] Our results are in agreement with this.

To summarize, we have presented two new water-soluble red/NIR- and blue-emitting molecular quantum clusters of silver. The UV/Vis, IR, luminescence, photoemission, XPS, XRD, and mass spectrometric characteristics of the clusters were reported. The Ag_8 cluster has strongly temperature and solvent sensitive luminescence. The temperature sensitivity of emission suggests applications. The results provide basic guidelines for further experimental and theoretical studies on the geometric and electronic structures, as well as the photophysical properties, of these clusters. Selective adsorption of Ag_8 clusters on metal oxides such as, Al_2O_3, TiO_2, and MgO suggests potential applications in catalysis. These clusters may be used in diverse studies in view of their facile phase transfer.

Experimental Section

About 85 mg of $AgNO_3$, dissolved in 1.693 mL water, was added to 448.9 mg of H_2MSA in 100 mL methanol under ice-cold conditions with vigorous stirring. Silver was reduced to the zero-valent state by slow addition of freshly prepared aqueous $NaBH_4$ solution (0.2 M, 25 mL). The reaction mixture was stirred for 1 h. The resulting precipitate was collected and repeatedly washed with methanol by centrifugal precipitation. Finally, the Ag@(H_2MSA) precipitate was dried and collected as a dark brown powder.

Interfacial etching was performed in an aqueous/organic biphasic system. H_2MSA thiol was partially dissolved in an organic solvent and parent Ag@(H_2MSA) was dispersed in the aqueous phase. Several organic solvents such as toluene, carbon tetrachloride, and diethyl ether can be used. The reaction products do not appear to be affected by varying the organic phase. An aqueous solution of the as-synthesized Ag@(H_2MSA) nanoparticles was added to an excess of H_2MSA in toluene (1/2 water/toluene ratio). A weight ratio of 1:3 was used (Ag@(H_2MSA):H_2MSA). The resulting mixture was stirred for 48 h at room temperature (ca. 303 K). Initiation of interfacial etching is indicated by the appearance of a blue layer at the interface after 0.5–1 h. As the reaction proceeds, the color of the aqueous phase changes from reddish brown to yellow and finally to orange. The reaction product was precipitated by addition of methanol and washed with methanol to remove excess H_2MSA. The product was freeze-dried and stored in the laboratory atmosphere.

PAGE separation of the clusters was performed as per the procedure given in Figure S1. Yields of Ag_8 and Ag_7 clusters obtained by continuous stirring for 48 h were 70 and 10 mg, respectively, starting from 100 mg Ag@MSA. Instrumental methods are given in Figure S1.

Received: December 17, 2009
Published online: April 20, 2010

Keywords: cluster compounds · interfacial reactions · luminescence · nanoparticles · silver

[1] P. A. Bartlett, B. Bauer, S. Singer, *J. Am. Chem. Soc.* **1978**, *100*, 5085–5089.
[2] C. E. Briant, B. R. C. Theobald, J. W. White, L. K. Bell, D. M. P. Mingos, A. Welch, *J. Chem. Soc. Chem. Commun.* **1981**, 201–202.

[3] G. Schmid, R. Pfeil, R. Boese, F. Bandermann, S. Meyer, G. H. M. Calis, J. W. A. vandervelden, *Chem. Ber.* **1981**, *114*, 3634 – 3642.

[4] a) J. Zheng, P. R. Nicovich, R. M. Dickson, *Annu. Rev. Phys. Chem.* **2007**, *58*, 409 – 431; b) J. Zheng, J. T. Petty, R. M. Dickson, *J. Am. Chem. Soc.* **2003**, *125*, 7780 – 7781; c) J. Zheng, C. W. Zhang, R. M. Dickson, *Phys. Rev. Lett.* **2004**, *93*, 077402; d) H. Duan, S. Nie, *J. Am. Chem. Soc.* **2007**, *129*, 2412 – 2413; e) M. A. Habeeb Muhammed, S. Ramesh, S. S. Sinha, S. K. Pal, T. Pradeep, *Nano Res.* **2008**, *1*, 333 – 340.

[5] P. Sevillano, O. Fuhr, O. Hampe, S. Lebedkin, E. Matern, D. Fenske, M. M. Kappes, *Inorg. Chem.* **2007**, *46*, 7294 – 7298.

[6] a) T. G. Schaaff, G. Knight, M. N. Shafi gullin, R. F. Borkman, R. L. Whetten, *J. Phys. Chem. B* **1998**, *102*, 10643 – 10646; b) Y. Shichibu, Y. Negishi, T. Tsukuda, T. Teranishi, *J. Am. Chem. Soc.* **2005**, *127*, 13464 – 13465; c) Y. Shichibu, Y. Negishi, H. Tsunoyama, M. Kanehara, T. Teranishi, T. Tsukuda, *Small* **2007**, *3*, 835 – 839; d) M. A. Habeeb Muhammed, T. Pradeep, *Chem. Phys. Lett.* **2007**, *449*, 186 – 190; e) E. S. Shibu, M. A. Habeeb Muhammed, T. Tsukuda, T. Pradeep, *J. Phys. Chem. C* **2008**, *112*, 12168 – 12176; f) M. A. Habeeb Muhammed, A. K. Shaw, S. K. Pal, T. Pradeep, *J. Phys. Chem. C* **2008**, *112*, 14324 – 14330; g) M. Zhu, E. Lanni, N. M. E. Garg, M. E. Bier, R. Jin, *J. Am. Chem. Soc.* **2008**, *130*, 1138 – 1139.

[7] O. Toikkanen, V. Ruiz, G. Ronnholm, N. Kalkkinen, P. Liljeroth, B. M. Quinn, *J. Am. Chem. Soc.* **2008**, *130*, 11049 – 11055.

[8] a) Y. Yanagimoto, Y. Negishi, H. Fujihara, T. Tsukuda, *J. Phys. Chem. B* **2006**, *110*, 11611 – 11614; b) G. H. Woehrle, M. G. Warner, J. E. Hutchison, *J. Phys. Chem. B* **2002**, *106*, 9979 – 9981; c) Y. Yang, S. Chen, *Nano Lett.* **2003**, *3*, 75 – 79; d) C. D. Grant, A. M. Schwartzberg, Y. Yang, S. Chen, J. Z. Zhang, *Chem. Phys. Lett.* **2004**, *383*, 31 – 34.

[9] M. A. H. Muhammed, P. K. Verma, S. K. Pal, R. C. ArunKumar, S. Paul, R. V. Omkumar, T. Pradeep, *Chem. Eur. J.* **2009**, *15*, 10110 – 10120.

[10] E. S. Shibu, B. Radha, P. K. Verma, P. Bhyrappa, G. U. Kulkarni, S. K. Pal, T. Pradeep, *ACS Appl. Mater. Interfaces* **2009**, *1*, 2199 – 2210.

[11] a) J. T. Petty, J. Zheng, N. V. Hud, R. M. Dickson, *J. Am. Chem. Soc.* **2004**, *126*, 5207 – 5212; b) J. G. Zhang, S. Q. Xu, E. Kumacheva, *Adv. Mater.* **2005**, *17*, 2336 – 2340; c) Z. Shen, H. Duan, H. Frey, *Adv. Mater.* **2007**, *19*, 349 – 352; d) A. Ledo-Suárez, J. Rivas, C. F. Rodrguez-Abreu, M. J. Rodrguez, E. Pastor, A. Hernndez-Creus, S. B. Oseroff, M. A. Lopez-Quintela, *Angew. Chem.* **2007**, *119*, 8979 – 8983; *Angew. Chem. Int. Ed.* **2007**, *46*, 8823 – 8827; e) S. N. Narayanan, S. K. Pal, *J. Phys. Chem. C* **2008**, *112*, 4874 – 4879; f) L. Shang, S. Dong, *Chem. Commun.* **2008**, 1088 – 1090; g) I. Díez, M. Pusa, S. Kulmala, H. Jiang, A. Walther, A. S. Goldmann, A. H. E. Muller, O. Ikkala, R. H. A. Ras, *Angew. Chem.* **2009**, *121*, 2156 – 2159; *Angew. Chem. Int. Ed.* **2009**, *48*, 2122 – 2125.

[12] a) M. R. Branham, A. D. Douglas, A. J. Mills, J. B. Tracy, P. S. White, R. W. Murray, *Langmuir* **2006**, *22*, 11376 – 11383; b) O. M. Bakr, V. Amendola, C. M. Aikens, W. Wenselers, R. Li, L. D. Negro, G. C. Schatz, F. Stellacci, *Angew. Chem.* **2009**, *121*, 6035 – 6040; *Angew. Chem. Int. Ed.* **2009**, *48*, 5921 – 5926.

[13] Z. Wu, E. Lanni, W. Chen, M. E. Bier, D. Ly, R. Jin, *J. Am. Chem. Soc.* **2009**, *131*, 16672 – 16674.

[14] a) N. Nishida, H. Yao, K. Kimura, *Langmuir* **2008**, *24*, 2759 – 2766; b) N. Nishida, H. Yao, T. Ueda, A. Sasaki, K. Kimura, *Chem. Mater.* **2007**, *19*, 2831 – 2841; c) N. Cathcart, P. Mistry, C. Makra, B. Pietrobon, N. Coombs, M. J. Niaraki, V. Kitaev, *Langmuir* **2009**, *25*, 5840 – 5846.

[15] a) X-J. Wang, T. Langetepe, C. Persau, B. Kang, G. M. Sheldrick, D. Fenske, *Angew. Chem.* **2002**, *114*, 3972 – 3977; *Angew. Chem. Int. Ed.* **2002**, *41*, 3818 – 3822; b) D. Fenske, C. Persau, S. Dehnen, C. E. Anson, *Angew. Chem.* **2004**, *116*, 309 – 313; *Angew. Chem. Int. Ed.* **2004**, *43*, 305 – 309; c) D. Fenske, C. E. Anson, A. Eichhfer, O. Fuhr, A. Ingendoh, C. Persau, C. Richert, *Angew. Chem.* **2005**, *117*, 5376 – 5381; *Angew. Chem. Int. Ed.* **2005**, *44*, 5242 – 5246; d) S. Chitsaz, D, Fenske, O, Fuhr, *Angew. Chem.* **2006**, *118*, 8224 – 8228; *Angew. Chem. Int. Ed.* **2006**, *45*, 8055 – 8059; e) C. E. Anson, A. Eichhfer, I. Issac, D. Fenske, O. Fuhr, P. Sevillano, C. Persau, D. Stalke, J. Zhang, *Angew. Chem.* **2008**, *120*, 1346 – 1351; *Angew. Chem. Int. Ed.* **2008**, *47*, 1326 – 1331.

[16] a) V. J. Catalano, H. Kar, J. Garnas, *Angew. Chem.* **1999**, *111*, 2083 – 2086; *Angew. Chem. Int. Ed.* **1999**, *38*, 1979 – 1982; b) T.-L. Hu, J.-R. Li, Y.-B. Xie, X.-H. Bu, *Cryst. Growth Des.* **2006**, *6*, 648 – 655; c) J.-X. Chen, Q.-F. Xu, Y. Xu, Y. Zhang, Z.-N. Chen, J.-P. Lang, *Eur. J. Inorg. Chem.* **2004**, 4247 – 4252.

[17] a) K. Matsumoto, R. Tanaka, R. Shimomura, Y. Nakao, *Inorg. Chim. Acta* **2000**, *304*, 293 – 296; b) K. Matsumoto, R. Tanaka, R. Shimomura, C. Matsumoto, Y. Nakao, *Inorg. Chim. Acta* **2001**, *322*, 125 – 129; c) K. Tang, X. Xie, L. Zhao, Y. Zhang, X. Jin, *Eur. J. Inorg. Chem.* **2004**, 78 – 85; d) O. M. Abu-Salah, M. H. Ja′far, A. R. Al-Ohaly, K. A. Al-Farhan, H. S. Al-Enzi, O. V. Dolomanov, J. A. K. Howard, *Eur. J. Inorg. Chem.* **2006**, 2353 – 2356.

[18] K. P. Kalayanikuttty, C. N. R. Rao, *Acc. Chem. Res.* **2008**, *41*, 489 – 499.

[19] S. H. Chen, K. Kimura, *Chem. Lett.* **1999**, *28*, 1169 – 1170.

[20] a) A. Dass, A. Stevenson, G. R. Dubay, J. B. Tracy, R. W. Murray, *J. Am. Chem. Soc.* **2008**, *130*, 5940 – 5946; b) T. G. Schaaff, R. L. Whetten, *J. Phys. Chem. B* **2000**, *104*, 2630 – 2641.

